

Document downloaded from:

<http://hdl.handle.net/10251/82714>

This paper must be cited as:

De-La-Torre, U.; Pereda-Ayo, B.; Moliner Marin, M.; González Velasco, JR.; Corma Canós, A. (2016). Cu-zeolite catalysts for NO<sub>x</sub> removal by selective catalytic reduction with NH<sub>3</sub> and coupled to NO storage/reduction monolith in diesel engine exhaust aftertreatment systems. *Applied Catalysis B: Environmental*. 187:419-427. doi:10.1016/j.apcatb.2016.01.020



The final publication is available at

<http://doi.org/10.1016/j.apcatb.2016.01.020>

Copyright Elsevier

Additional Information

# Cu-zeolite Catalysts for NO<sub>x</sub> Removal by Selective Catalytic Reduction with NH<sub>3</sub> and Coupled to NO<sub>x</sub> Storage/reduction Monolith in Diesel Engine Exhaust Aftertreatment Systems

*Unai De-La-Torre,<sup>†</sup> Beñat Pereda-Ayo,<sup>†</sup> Manuel Moliner,<sup>‡</sup> Juan R. González-Velasco<sup>\*†</sup>,  
Avelino Corma<sup>\*‡</sup>*

<sup>†</sup>Departamento de Ingeniería Química, Facultad de Ciencia y Tecnología, Universidad del País Vasco/Euskal Herriko Unibertsitatea (UPV/EHU), P.O. Box 644, 48080 Bilbao, Bizkaia, Spain.

<sup>‡</sup>Instituto de Tecnología Química, Universidad Politécnica de Valencia, Consejo Superior de Investigaciones Científicas, Avenida de los Naranjos s/n, 46022 Valencia, Spain.

KEYWORDS: Cu-zeolite, Cu-chabazite, SCR, NSR-SCR, NO<sub>x</sub> removal

ABSTRACT: Coupled NSR-SCR systems comprising a Pt-BaO/Al<sub>2</sub>O<sub>3</sub> NSR monolith and Cu/CHA, Cu/ZSM-5 or Cu/BETA SCR catalysts are prepared and tested for NO<sub>x</sub> removal from diesel and lean burn engines exhaust gases. The Cu/zeolite catalysts are characterized by ICP-AES, XRD, N<sub>2</sub> adsorption-desorption, NH<sub>3</sub>-TPD and H<sub>2</sub>-TPR. The physico-chemical characteristics of fresh catalysts and aged under 5% steam/Ar at 750 °C for 16 h and are compared, resulting in the Cu/CHA with much higher hydrothermal resistance to the loss of

textural and structural properties. The single-SCR, single-NSR and coupled NSR-SCR catalytic performance is studied including the conversion of NO and NH<sub>3</sub>, slip of NH<sub>3</sub>, and N<sub>2</sub>O and NO<sub>2</sub> yields. Cu/CHA presents the SCR wider temperature window, eventually 100% NO conversion from 220 to 380 °C, even maintained after severe aging. For application in the NSR-SCR technology, the NH<sub>3</sub> generated in the NSR catalyst during the rich period is able to achieve higher NO conversion reducing significantly the slip of NH<sub>3</sub> (negligible at 200 °C and above), very few amount of N<sub>2</sub>O at any temperature, and small production of NO<sub>2</sub> only at higher temperatures. This improvement of activity and selectivity is particularly enhanced with the coupled NSR-Cu/CHA system, which is also maintained when the catalyst is deposited on the cordierite monolith substrate, as in the case of real application.

## INTRODUCTION

Diesel engines and lean burn engines are more fuel combustion efficient and generate less CO<sub>2</sub> emissions compared with traditional stoichiometric engines. However, the excess of oxygen of diesel and lean burn exhaust makes difficult the chemical reduction of NO<sub>x</sub> (preferentially to N<sub>2</sub>), and NO<sub>x</sub> removal remains as a challenge for automobile emission reduction. Lean NO<sub>x</sub> traps (LNTs) —also denominated NO<sub>x</sub> storage and reduction (NSR) catalysts— and selective catalytic reduction (SCR) have been developed over the past 15 years as two promising technologies to overcome this problem.<sup>1</sup>

Basically, NSR catalysts consist of an alkali or alkali-earth oxide (e.g. BaO) and a noble metal (Pt) impregnated on alumina.<sup>2-4</sup> These catalysts operate under cyclic oxidizing-reducing conditions. During the lean period, when oxygen is in excess, platinum oxidizes NO to a mixture of NO and NO<sub>2</sub> (NO<sub>x</sub>), which is adsorbed (stored) on Ba as various NO<sub>x</sub> species (nitrate, nitrite). During the subsequent short rich period, when some reductant (e.g. H<sub>2</sub> or

hydrocarbon from the fuel) is injected, NO<sub>x</sub> ad-species are released and reduced to nitrogen on Pt. In contrast to NSR catalysts, SCR systems rely upon the catalyzed reaction of NO<sub>x</sub> with externally added NH<sub>3</sub> over Fe or Cu/zeolite without precious metal.<sup>5-7</sup>

More recently, emissions treatment systems with a lean NO<sub>x</sub> trap (LNT) as the ammonia-generating device, which also provides functionality for NO<sub>x</sub> removal, and an SCR catalyst disposed downstream of the ammonia-generating device have been proposed, firstly patented by researchers at Ford Motor Co.<sup>8</sup> The working principle of the coupled LNT-SCR system is as follows: During the rich phase, part of the NO<sub>x</sub> stored on the LNT in the previous lean phase is reduced selectively to NH<sub>3</sub>, which is then stored in the downstream SCR unit. NH<sub>3</sub> trapped by the acidic sites of the metal-exchanged zeolite is utilized to reduce NO<sub>x</sub> that slips from the LNT during the subsequent lean phase. The objective is to generate in the LNT as much NH<sub>3</sub> as needed to completely reduce NO<sub>x</sub>, releasing to the atmosphere only innocuous compounds, such as nitrogen and water. Hence, in the coupled NSR-SCR systems not only is the NO<sub>x</sub> removal efficiency greatly increased but also the NH<sub>3</sub> slip is significantly decreased.<sup>9-12</sup> In addition, the presence of the SCR catalyst reduces the N<sub>2</sub>O emissions (formed on the LNT). This catalytic technology has been applied in the US and Europe by Daimler AG.<sup>9</sup>

One of the major issues of NH<sub>3</sub>-SCR catalysts is activity loss due to thermal degradation, becoming hydrothermal stability of Cu/zeolites a crucial issue for this application.<sup>13</sup> High temperatures can be found quite frequently in commercial applications when LNTs are placed upstream of the SCR catalyst. Thus, attention has shifted from large and medium pore zeolites (ZSM-5 and BETA) to include small-pore Cu-exchanged chabazite (Cu/CHA), such as Cu/SSZ-13 and Cu/SAPO-34 which are stable after steaming at 800 °C.<sup>14-17</sup> Different types/locations of Cu species have been observed on Cu/zeolite catalysts, such as isolated Cu<sup>2+</sup>, Cu<sup>+</sup>, Cu dimers (Cu-O-Cu)<sup>2+</sup>, Cu<sub>x</sub>O<sub>y</sub> clusters, and CuO particles.<sup>17-19</sup> However, unlike

**Comentario [MMM1]:** Añadir si es posible las siguientes referencias:  
-R. Martínez-Franco, M. Moliner, P. Concepcion, J. R. Thogersen, A. Corma, J. Catal., 2014, 314, 73  
- N. Martín, M. Moliner, A. Corma, Chem. Commun., 2015, 51, 9965

hydrothermally treated Cu/ZSM-5 and Cu/BETA catalysts, minor changes in the copper sites were observed on Cu/SSZ-13, which was consistent with the minor changes in the SCR activity of the Cu/SSZ-13 catalyst after the hydrothermal treatment process.<sup>20</sup> Recently, Wang et al.<sup>21</sup> found that over Cu/SSZ-13, initial aging at 750 °C results in increased NH<sub>3</sub> oxidation and selectivity to NO<sub>x</sub>, suggesting the aggregation of isolated Cu<sup>2+</sup> sites into CuO particles, while further aging at 800 °C leads to decreased NH<sub>3</sub> oxidation activity due to structure collapse. On the other hand, for Cu/SAPO-34, they did not find any significant change in NH<sub>3</sub> oxidation after hydrothermal aging. Most of these studies were carried out with Cu/zeolites in its powdered or granulated form. Only Ma et al.<sup>22</sup> studied fully formulated washcoat cordierite monoliths purchased from the major catalyst suppliers and tested them after hydrothermal aging at 600, 750 and 850 °C in simulated exhaust gases containing water.

On the other hand, few studies have appeared concerning the effect of aging on the performance of LNT-SCR systems. Seo et al.<sup>23</sup> examined the deNO<sub>x</sub> characteristics of coupled Pt/Pd/Rh LNT and Fe/zeolite SCR catalysts using CO/H<sub>2</sub> as reductant, the LNT-SCR system being subjected to hydrothermal aging. McCabe et al.<sup>10,24</sup> examined the performance of systems incorporating Fe/zeolite and Cu/zeolite catalysts. It was concluded that the SCR catalyst was able to compensate the decreased NO<sub>x</sub> reduction after aging. Recently, Wang et al.<sup>25</sup> studied the effect of simulated road aging on the NO<sub>x</sub> reduction performance of coupled Pt/Rh and Cu/CHA SCR catalysts supplied by BASF prepared on ceramic monoliths, and using H<sub>2</sub>, CO and C<sub>3</sub>H<sub>6</sub> as NO<sub>x</sub> reductants.

The present study aims to evaluate the performance of coupled LNT-SCR systems comprising a low Pt LNT and a Cu/ZSM-5, Cu/BETA or Cu/CHA SCR catalyst, tested in their granulated form and also prepared and tested on 400 cpsi ceramic monoliths, fresh and after simulated road aging. NO<sub>x</sub> conversion and NH<sub>3</sub> production and N<sub>2</sub>O emissions from the

**Comentario [MMM2]:** Añadir si es posible la referencia anterior:  
-N. Martín, M. Moliner, A. Corma, Chem. Commun., 2015, 51, 9965

LNT and from the coupled LNT-SCR system are reported, and an effort is made to relate changes in catalytic performance after aging to changes in the structure of the catalysts.

## EXPERIMENTAL SECTION

**Preparation of powdered chabazite.** First, N,N,N-trimethyl-1-adamantammonium (TMAda) was prepared for its use as organic structure directing agent (OSDA) in the synthesis of chabazite. For this purpose, 29.6 g of 1-Adamantamine (Sigma-Aldrich) and 64 g of potassium carbonate (Sigma-Aldrich) were mixed with 320 ml of chloroform. Then, 75 g of methyl iodide was added dropwise while the reaction was stirred in an ice bath. The reaction was maintained for 5 days under agitation at room temperature. The mixture were filtered and washed with diethyl ether, and the resultant solid further extracted with chloroform. The final product was N,N,N-trimethyl-1-adamantammonium iodide. This iodide salt was anion exchanged using an ion exchange resin, and finally, an aqueous solution of the hydroxide form of TMAda was achieved (7.6%wt).

Chabazite zeolite was prepared following the former synthesis description reported by Zones.<sup>26</sup> In this sense, 1.45 g of sodium hydroxide (Sigma-Aldrich, 98%) was dissolved in 99.9 g of an aqueous solution of N,N,N-trimethyl-1-adamantammonium hydroxide (7.6%wt), and the mixture was maintained under stirring for 15 minutes. Then, 1.0 g of aluminum hydroxide (66%wt, Sigma-Aldrich) and 10.9 g of fumed silica (aerosil) were introduced in the synthesis mixture, and maintained under stirring the required time to evaporate the solvent until the desired gel concentration. The final gel composition was  $\text{SiO}_2 : 0.037 \text{ Al}_2\text{O}_3 : 0.20 \text{ TMAda} : 0.20 \text{ NaOH} : 18.3 \text{ H}_2\text{O}$ . The gel was transferred to an autoclave with a Teflon liner, and heated at 150°C for 5 days under dynamic conditions. The sample after

hydrothermal crystallization was filtered and washed with abundant distilled water, and finally dried at 100 °C. Finally, CHA zeolite was calcined at 580 °C for 4 h.

**Cu-exchanged zeolites as SCR catalysts.** Ion exchange (IE) was the method used for preparing the Cu-exchanged zeolites. Beta and ZSM-5 zeolites were ion exchanged using an aqueous solution of  $\text{Cu}(\text{COOCH}_3)_2$  (Panreac, 98%) containing the required amount of Cu. The solid to liquid ratio for the IE was fixed at 8g/L, and the resultant mixture was maintained under stirring for 24 h at 65 °C. The ion exchanged zeolites were then filtered, washed twice with deionized water, dried overnight at 110 °C and calcined at 550 °C for 4 h. Catalysts with other copper loadings were also prepared, between 1 and 6 wt.%,<sup>19</sup> being chosen for this investigation the nominal copper loading of 4-5% for Cu/BETA and Cu/ZSM-5 catalysts, as they achieved higher DeNO<sub>x</sub> efficiency. In order to perform the Cu ion exchange on the calcined CHA zeolite, the sample was first washed with a 0.04 M aqueous solution of  $\text{NaNO}_3$  (~150 ml/ g of zeolite). Then, the Cu IE was conducted using an aqueous solution of  $\text{Cu}(\text{CH}_3\text{CO}_2)_2$  containing the required amount of Cu. The liquid to solid ratio was fixed at 100ml/g of zeolite, and the resultant mixture was maintained under stirring overnight at room temperature. Finally, the sample was filtered and washed with distilled water, and calcined at 550°C for 4 h. The prepared powdered catalysts were then pelletized, crushed and sieved to 0.3-0.5 mm. Previous experiments carried out with different particle size catalysts revealed that mass transfer limitations could be considered negligible, so that internal diffusion in the catalyst particle was not the rate-controlling step in the kinetic mechanism for this particle size of 0.3-0.5 mm.

The actual chemical compositions of the Cu-exchanged zeolites, as well as the nomenclature used in the manuscript, are summarized in **Table 1** (granulated).

**Table 1.** The prepared catalysts.

Zeolite	Si/Al	Granulated		Monoliths		
		Denomination	Cu wt%	Denomination	Washcoat weight, g	Cu content, % (related to washcoat)
BETA	12.5	Cu/BETA	2.1	Cu/BETA/M	1.04	4.9
ZSM-5	25.0	Cu/ZSM-5	1.9	Cu/ZSM-5/M	1.31	5.4
CHABAZITE	10.6	Cu/CHA	3.9	Cu/CHA/M	1.08	3.9

**SCR monolith preparation.** Several 20 mm in length and 20 mm diameter monoliths of cordierite ( $2\text{Al}_2\text{O}_3 \cdot 5\text{SiO}_2 \cdot 2\text{MgO}$ ), i.e. a volume of  $6.28 \text{ cm}^3$ , were cut from a bigger commercial sample supplied by Corning, with a cell density of 400 cpsi,  $1 \text{ mm}^2$  square channels and wall thickness of  $150 \mu\text{m}$ , to be used as substrates. After calcination in air at  $700 \text{ }^\circ\text{C}$  to remove possible impurities, the Cu/zeolite SCR-monoliths were prepared by washcoating cordierite monoliths with powder Cu/zeolites. The most relevant details of the preparation procedure of copper-zeolite catalysts were described elsewhere.<sup>27</sup>

The washcoating of cordierite monoliths was carried out by slurry dip-coating. In the case of Cu/ZSM-5 and Cu/BETA powders, the solid content of the slurry was adjusted to 40% by adding the required amount of water, while the solid content was 20% for Cu/CHA. The actual Cu content of powder Cu/ZSM-5 and Cu/BETA catalysts to be used as washcoat in cordierite monoliths were previously determined,<sup>27</sup> resulting in values close to 5% in both cases, while for the case of Cu/CHA, 3.9 wt.% Cu granulated catalyst was finally used as the washcoat. Then, the slurries were milled with ceramic balls for 16 h until homogeneous slurry was obtained. After ball milling, 10 wt.% colloidal silica (Ludox-HS 40, Sigma-Aldrich) was added in order to enhance the mechanical stability and the adherence of the washcoat to cordierite. The washcoating was made by immersion of the monoliths into the corresponding slurry for 3 min; afterwards the excess of liquid retained in the channels was



blown out with compressed air and the monoliths were dried at 110 °C for 30 min. This procedure was repeated until c.a. 1 g of Cu/BETA, Cu/ZSM-5 or Cu/CHA was washcoated. Finally, the monoliths were calcined at 550 °C for 4 h.

Among other monolith catalysts prepared with different copper loading in the washcoat, those reported in Table 1 (monoliths) resulted in the best DeNO<sub>x</sub> performance and thus chosen for this investigation.

**NSR monolith preparation.** The Pt-BaO/Al<sub>2</sub>O<sub>3</sub> NSR monolith catalyst was prepared according to our previously reported procedure.<sup>28</sup> In summary, a cordierite monolith, 20 mm in length and diameter, with a cell density of 400 cpsi and a wall thickness of 150 μm was washcoated with γ-alumina (163 m<sup>2</sup> g<sup>-1</sup> after stabilization at 700 °C, 4h) by several immersions of the monolith into the alumina slurry until c.a. 1 g Al<sub>2</sub>O<sub>3</sub> was deposited in the monolith structure. The incorporation of platinum was achieved by adsorption from tetraammine platinum (II) nitrate solution and the excess of liquid remaining in the channels was blown out with compressed air. After calcination in air (500 °C, 4 h) and subsequent reduction of the metallic phase in a 5% H<sub>2</sub>/N<sub>2</sub> stream (500 °C, 1h), the barium was incorporated by immersion of the monolith in a barium acetate solution. Finally, the catalyst was calcined again (500 °C, 4h).

**Aging procedure.** For the hydrothermal aging studies, the SCR catalysts in their granulated form were aged under 5% H<sub>2</sub>O in Ar at 750 °C for 16 h, at a total flow rate of 600 ml min<sup>-1</sup>.

**Characterization techniques.** The prepared catalysts were characterized by the appropriate equipments and techniques, as specified in the Supporting Information: actual amount of copper by Inductively Coupled Plasma Atomic Emission Spectroscopy (ICP-AES), crystalline structure of zeolites by X-Ray Diffraction (XRD), surface area and porosity by N<sub>2</sub> adsorption-desorption at -196 °C, acidic properties by NH<sub>3</sub> Temperature Programmed

Desorption (NH<sub>3</sub>-TPD), and reducibility of Cu species by Hydrogen Temperature Programmed Reduction (H<sub>2</sub>-TPR). Details on the analysis equipment are given in the Supporting Information.

**Activity tests: selective catalytic reduction (SCR).** The SCR experiments were performed in a downflow stainless steel reactor. The reactor tube was located into a 3-zone tube furnace, where the monolith or 1 g of 0.3-0.5 mm pelletized catalyst was placed. The temperature was measured by a thermocouple at the top of the monolith/catalyst bed. The reaction temperature was varied from 140 to 500 °C for powdered catalysts and 150 to 400 °C for monolithic catalysts, in steps of 50 °C. The composition of the feed gas mixture was 750 ppm NO, 750 ppm NH<sub>3</sub> and 6% O<sub>2</sub> using Ar as the balance gas. Gases were fed via mass flow controllers and the total flow rate was set at 3,000 ml min<sup>-1</sup>, which corresponded to a space velocity (GHSV) of 90,000 h<sup>-1</sup> (28,600 h<sup>-1</sup> with monolith). The experimental setup was designed to minimize the gas phase oxidation of NO to NO<sub>2</sub>, and therefore, the NO<sub>2</sub> concentration in the gas fed is almost null. The NO, NO<sub>2</sub>, NH<sub>3</sub> and N<sub>2</sub>O concentrations at the reactor exit were monitored every 40 °C, once the gas composition has been stabilized for at least 10 min, by an online FTIR multigas analyzer (MKS 2030).

The NO ( $X_{NO}$ ) and NH<sub>3</sub> ( $X_{NH_3}$ ) conversions were calculated as

$$X_{NO} = \frac{F_{NO}^{in} - F_{NO}^{out}}{F_{NO}^{in}} \times 100 \quad (1)$$

$$X_{NH_3} = \frac{F_{NH_3}^{in} - F_{NH_3}^{out}}{F_{NH_3}^{in}} \times 100 \quad (2)$$

and the N<sub>2</sub>, NO<sub>2</sub> and N<sub>2</sub>O selectivities, named  $S_{N_2}$ ,  $S_{NO_2}$  and  $S_{N_2O}$  respectively, were calculated as

$$S_{N_2} = \frac{2F_{N_2}^{out}}{F_{NH_3}^{in} X_{NH_3} + F_{NO}^{in} X_{NO}} \times 100 \quad (3)$$

$$S_{NO_2} = \frac{F_{NO_2}^{out}}{F_{NH_3}^{in} X_{NH_3} + F_{NO}^{in} X_{NO}} \times 100 \quad (4)$$

$$S_{N_2O} = \frac{2F_{N_2O}^{out}}{F_{NH_3}^{in} X_{NH_3} + F_{NO}^{in} X_{NO}} \times 100 \quad (5)$$

where  $F_i$  represents the concentration of the “i” species and the superscripts “in” and “out” indicate that the gas concentration was referred to the inlet and the exit of the reactor, respectively.

**Activity tests: Coupled NSR-SCR configuration.** The  $NO_x$  storage–reduction experiments for the single NSR configuration were performed in a vertical downflow stainless steel reactor, inside which the Pt-BaO/Al<sub>2</sub>O<sub>3</sub> monolith was placed. When testing the coupled NSR-SCR configuration, the SCR pelletized or monolith catalyst was packed in a second reactor connected downstream the NSR reactor. Temperature was measured by thermocouples at the top of the NSR monolith, and in the top of the monolith and top part of the bed of SCR catalyst. Streams from either the exit of the NSR monolith or the exit of the coupled NSR–SCR system can be alternatively addressed to analyzers.

This system was run under cycled NSR conditions alternating long lean and short rich periods. The composition of the lean gas mixture for  $NO_x$  storage was 750 ppm NO and 6% O<sub>2</sub> using Ar as balance gas. During the rich period oxygen was replaced by 4% hydrogen maintaining 750 ppm of NO in the feedstream. The duration of the lean and rich period ( $t_L = 150$  s and  $t_R = 20$  s, respectively) was maintained constant and controlled by two solenoid valves. Gases were fed via mass flow controllers and the total flowrate was set at 3,000 ml min<sup>-1</sup>, which corresponded to a GHSV of 90,000 or 28,600 h<sup>-1</sup> (granulated or monolith, respectively) for either NSR or SCR catalysts.  $NO_x$  storage and reduction tests were carried out varying the catalyst temperature from 140 to 420 °C. The objective was to maximize the production of N<sub>2</sub>, with minimum NH<sub>3</sub>, NO, NO<sub>2</sub> and N<sub>2</sub>O at the exit. Following are the expressions to calculate yields:

$$Y_{\text{NH}_3} = \frac{\text{NH}_3^{\text{out}}}{(\text{NO}^{\text{in}})_{\text{L}} + (\text{NO}^{\text{in}})_{\text{R}}} \times 100 = \frac{\int_0^{t_L+t_R} F_{\text{NH}_3}^{\text{out}} dt}{F_{\text{NO}}^{\text{in}}(t_L+t_R)} \times 100 \quad (6)$$

$$Y_{\text{N}_2} = \frac{2\text{N}_2^{\text{out}}}{(\text{NO}^{\text{in}})_{\text{L}} + (\text{NO}^{\text{in}})_{\text{R}}} \times 100 = \frac{\int_0^{t_L+t_R} 2F_{\text{N}_2}^{\text{out}} dt}{F_{\text{NO}}^{\text{in}}(t_L+t_R)} \times 100 \quad (7)$$

$$Y_{\text{N}_2\text{O}} = \frac{2\text{N}_2\text{O}^{\text{out}}}{(\text{NO}^{\text{in}})_{\text{L}} + (\text{NO}^{\text{in}})_{\text{R}}} \times 100 = \frac{\int_0^{t_L+t_R} 2F_{\text{N}_2\text{O}}^{\text{out}} dt}{F_{\text{NO}}^{\text{in}}(t_L+t_R)} \times 100 \quad (8)$$

$$Y_{\text{NO}_2} = \frac{\text{NO}_2^{\text{out}}}{(\text{NO}^{\text{in}})_{\text{L}} + (\text{NO}^{\text{in}})_{\text{R}}} \times 100 = \frac{\int_0^{t_L+t_R} F_{\text{NO}_2}^{\text{out}} dt}{F_{\text{NO}}^{\text{in}}(t_L+t_R)} \times 100 \quad (9)$$

## RESULTS AND DISCUSSION

**SCR catalysts characterization.** Figure S1 (Supporting Information) displays the XRD patterns recorded for the fresh (continuous line) and hydrothermally aged (dashed line) samples, which demonstrate that the catalysts have CHA, BEA and MFI structures. No peaks related to CuO and Cu<sub>2</sub>O are observed in any case, suggesting that the Cu is highly dispersed or the formed Cu<sup>2+</sup> complex is not large enough to be detected by XRD. No collapse of the catalytic structure even after hydrothermal aging, i.e. zeolite structures remained largely intact even during harsh conditions, with the exception of Cu/BETA that losses some crystallinity after the hydrothermal treatment. In the case of CHA framework, the aluminum hydroxide species [Al(OH)<sub>3</sub>] formed during dealumination at high temperature hydrothermal conditions, are reattached back to the framework when zeolite is subsequently cooled, maintaining the integrity of the structure.

The N<sub>2</sub> adsorption-desorption isotherms of the Cu-exchanged zeolites in their fresh and aged forms are shown in Figure S2 (Supporting Information). Numerical treatment of N<sub>2</sub> isotherms provides BET surface area and pore volume reported in **Table 2**. The aging process results in a partial decrease of the surface area and micropore volume for all samples, in

agreement with recently reported results.<sup>29</sup> The surface area decrease results in about 28% for Cu/BETA and Cu/ZSM-5, but only 17% in the case of Cu/CHA, the latter even with much higher initial value. Similar trend is found for micropore volume decrease ZSM-5 > BETA > CHA.

**Table 2.** Physico-chemical properties of the powdered catalysts, fresh and after severe hydrothermal aging under 5% H<sub>2</sub>O/Ar at 750 °C for 16 h, at a total flow rate of 600 ml min<sup>-1</sup>.

Catalyst	Surface area, m <sup>2</sup> g <sup>-1</sup>		Pore vol. (micro), mm <sup>3</sup> g <sup>-1</sup>		Acidity, μmol NH <sub>3</sub> g <sup>-1</sup>		Reducibility, μmol H <sub>2</sub> g <sup>-1</sup>	
	Fresh	Aged	Fresh	Aged	Fresh	Aged	Fresh	Aged
Cu/BETA	501	362	203 (148)	165 (98)	100	46.2	268	291
Cu/ZSM-5	381	274	210 (106)	179 (48)	68.7	49.9	792	704
Cu/CHA	579	481	287 (245)	248 (207)	135	121	1061	992

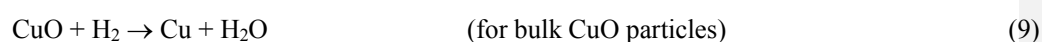
The amount of ammonia uptake is reported in Table 2, determined from ammonia desorption profiles over Cu/zeolite catalysts measured by NH<sub>3</sub>-TPD (Figure S3 in the Supporting Information). The strength of acid sites of the zeolites is given by the relative position of the ammonia desorption peaks with respect to temperature in the NH<sub>3</sub>-TPD curves. First peak represents the adsorbed NH<sub>3</sub> molecules at weak Brønsted acid sites and weak Lewis acid sites related to Cu species, while the latter at the highest temperature represents the adsorbed NH<sub>3</sub> both on strong Brønsted acid sites of zeolite and new Lewis acid sites created by the Cu species.<sup>30</sup>

Also the effect of the thermal aging on the acidity of the different Cu-exchanged zeolites can be analyzed by comparison of values in Table 2. Fresh catalysts show different amount of adsorbed NH<sub>3</sub> molecules, resulting in 3.31, 2.44 and 1.68 ml NH<sub>3</sub> for Cu/CHA, Cu/BETA and Cu/ZSM-5, respectively. After the aging treatment, the catalyst with minor changes was

again Cu/CHA (11% vs. 27% and 54% for Cu/ZSM-5 and Cu/BETA, respectively). Interestingly, the moderate acidity, corresponding to the NH<sub>3</sub> desorption peak centered at ~250 °C, remains unaltered for the aged Cu/CHA catalyst, probably due to its lower dealumination.

Additional information about the nature of different copper species in the catalysts was obtained by H<sub>2</sub>-TPR experiments (Figure S4 in Supporting Information), from which the H<sub>2</sub> consumption before and after the hydrothermal treatment can be calculated and are given in Table 2. The copper-free H-zeolites did not contain reducible ions and no H<sub>2</sub> consumption was noticed; therefore, all H<sub>2</sub> consumed by the catalysts can be attributed to the reduction of copper cations.

Considering the ICP-AES copper content, the amount of catalyst sample used in the H<sub>2</sub>-TPR experiments and the stoichiometry of the following reactions:



a ratio H<sub>2</sub>/Cu = 1 should be obtained if all copper species were Cu(II) and if all Cu(II) species were completely reduced to metal copper. It is important to note that the H<sub>2</sub>/Cu ratios achieved experimentally were 0.9–1.0 in all cases, which confirms that Cu(II) species are mostly abundant on the catalysts.

The H<sub>2</sub> consumption peaks from 100 °C to 1000 °C correspond to several copper species presenting different reducibility, which in total are not so different before and after the ageing process (Table 2). However, the aging process seems to introduce remarkable changes in the copper species distribution depending on the zeolite structure. In Figure S4, it can be observed that the hydrogen consumption profile of the Cu/CHA remains almost unaltered before and after ageing. In contrast, Cu/ZSM-5 and Cu/BETA catalysts show enlargement of the peak close to 600 °C (reduction of Cu(II) cations in octahedral coordination) at the

expense of reduction of the peak around 300 °C (easily reduced Cu(II) exchanged species), probably by migration of tetracoordinated Cu to Cu in octahedral coordination during the high temperature hydrothermal treatment.<sup>22</sup>

**SCR reactions with granulated Cu/zeolite.** Figure 1 shows NO and NH<sub>3</sub> conversions as well as selectivity towards N<sub>2</sub>, as a function of the reaction temperature in SCR experiments with catalysts in their granulated form. As seen, NO conversions increased with temperature as the NO<sub>x</sub> NH<sub>3</sub>-SCR reaction is promoted, reaching a maximum at intermediate temperatures and decreasing afterwards as the oxidation of ammonia with O<sub>2</sub> is favored at higher temperatures.<sup>31</sup> NH<sub>3</sub> conversion also increases with temperature, but 100% conversion was maintained above certain temperature where the NH<sub>3</sub>-O<sub>2</sub> reaction prevails. The minimum temperature for 100% ammonia conversion is coincident with that of maximum NO conversion. Regardless the catalyst, N<sub>2</sub> is almost the only reaction product and very few N<sub>2</sub>O and/or NO<sub>2</sub> are detected.

---

**Figure 1.** NO conversion, NH<sub>3</sub> conversion and N<sub>2</sub> selectivity during SCR reaction for the catalysts, in their granulated form (fixed bed reactor).

---

Among the studied catalysts, undoubtedly, Cu/CHA results in the best catalytic performance, due to the higher NO conversion achieved between 140-380 °C (almost 100% from 220 to 380 °C) and slightly higher N<sub>2</sub> selectivity compared to Cu/BETA and Cu/ZSM-5 catalysts. Also Cu/CHA provides the higher consumption of ammonia, minimizing then the NH<sub>3</sub> slip in the system. On the other hand, Cu/ZSM-5 achieved higher NO conversion than Cu/BETA in the temperature range of 180-380 °C and higher NH<sub>3</sub> consumption in the whole range. Only at temperature above 380 °C, Cu/BETA achieves better NO conversion.

The effect of the presence of water in the feedstream on the NH<sub>3</sub>-SCR reaction has also been studied. **Figures 2a, 2b** and **2c** show the NO and NH<sub>3</sub> conversions and selectivity towards N<sub>2</sub> with reaction temperature for Cu/CHA, Cu/BETA and Cu/ZSM-5 catalysts, respectively, in the absence (black lines) and presence of water (red lines). The presence of water improves catalytic behavior of all prepared catalysts, especially at higher reaction temperatures, probably due to an inhibition effect of water over the ammonia oxidation, which is the reaction prevailing at temperatures over 400 °C. However, the effect of water at low reaction temperatures remains unclear in the literature. In fact, some authors<sup>32</sup> claimed that water inhibits NO oxidation to NO<sub>2</sub> (rate-determining reaction), and equilibrium is thermodynamically displaced towards formation of NO, whereas others<sup>33</sup> reported the enhancement of the catalytic activity in the presence of water. Interestingly, NO conversion is slightly improved with Cu/BETA at lower reaction temperatures, between 180-260 °C. All catalysts show an improvement of N<sub>2</sub> selectivity at higher reaction temperatures, whereas small differences are observed for low-medium reaction temperatures.

---

**Figure 2.** Conversion of NO, NH<sub>3</sub> and N<sub>2</sub> selectivity during SCR reaction for the catalysts in their granulated form in the absence (black) and presence (red) of water in the feed for a) Cu/CHA, b) Cu/BETA and c) Cu/ZSM-5 catalysts.

---

**SCR aging.** Due to the importance of the H<sub>2</sub>O resistance of catalysts for the SCR reaction, the catalytic activity of the aged Cu-containing catalysts has been evaluated. Cu/CHA, Cu/ZSM-5 and Cu/BETA powders were submitted to a severe aging process by treating them with 5% H<sub>2</sub>O in Ar at 750 °C for 16 h. **Figures 3a, 3b** and **3c** show the NO and NH<sub>3</sub>



conversions and  $N_2$ ,  $N_2O$  and  $NO_2$  selectivities for fresh (black lines) and aged (red lines) catalysts, as a function of the reaction temperature in SCR experiments.

---

**Figure 3.** Conversion of NO,  $NH_3$  and selectivity of  $N_2$ ,  $N_2O$  and  $NO_2$  during SCR reaction for fresh (black) and aged (red) granulated catalysts a) Cu/CHA, b) Cu/BETA and c) Cu/ZSM-5.

---

In the comparison between fresh and aged catalyst, the most notorious fact for Cu/CHA (Figure 3a) is the decrease in the NO conversion at temperatures above 380 °C when the catalyst has been harshly aged. NO removal decreases around 40% between 420 and 500 °C. This effect could be related to the partial loss of some physico-chemical characteristics of this catalyst, such as acidity and micropore volume. This fact could also produce the decrease in  $N_2$  selectivity (10% loss), due to a promotion of  $N_2O$  production at intermediate temperatures and  $NO_2$  at higher temperatures.

On the other hand, the hydrothermal treatment causes a dramatic decrease in the catalytic performance of Cu/BETA and Cu/ZSM-5 (Figures 3b and 3c, respectively). Indeed, Cu/BETA shows NO conversions below 50%, and Cu/ZSM-5 only achieves 75% NO conversion at 380 °C. In addition, Cu/BETA and Cu/ZSM-5 catalysts also form higher amount of  $N_2O$  at intermediate temperatures and  $NO_2$  at higher temperatures, especially Cu/ZSM-5, which achieves 12% selectivity towards  $NO_2$  above 420 °C. This poorer catalytic performance at higher temperatures is probably related to the loss of specific surface, acidity and reducibility of the catalysts, as previously explained.

**SCR reactions in the monolithic form.** Figure 4 shows the NO and  $NH_3$  conversions as well as  $N_2$ ,  $N_2O$  and  $NO_2$  selectivities, with reaction temperature in SCR experiments for the

catalysts in their monolithic form. The performance of Cu/CHA/M is also shown when 5% of water was added to the feedstream (dashed lines).

---

**Figure 4.** Conversion of NO and NH<sub>3</sub> (two upper graphics) and selectivity of N<sub>2</sub>, N<sub>2</sub>O and NO<sub>2</sub> (three bottom graphics) during SCR reaction for the prepared monoliths.

---

As seen in Figure 4, Cu/CHA/M shows the best catalytic behavior compared to Cu/BETA/M and Cu/ZSM-5/M catalysts. Cu/CHA/M achieves a maximum NO conversion of 98% at 260 °C, and NO conversion values above 80% within 220-320 °C, regardless the presence or absence of water in the feedstream. It is worth to note that at higher temperatures the NO removal is significantly improved when water is present in the feedstream. These results reveal a significant catalytic improvement of chabazite catalyst compared to the other conventional zeolites, whose NO conversions are below 80% within the whole studied temperature range. Indeed, the maximum NO conversions for ZSM-5 and BETA monoliths were 80% and 60%, respectively.

Furthermore, Cu/CHA/M gave maximum N<sub>2</sub> selectivity, even better when water is present in the feedstream. High N<sub>2</sub> selectivity values (~ 98%) are achieved at low temperatures (~140 °C), whereas a gradual decrease of the N<sub>2</sub> selectivity is observed when increasing the reaction temperature (80% at 380 °C, see Figure 4c). On the other hand, selectivity towards N<sub>2</sub>O increases progressively from negligible at 140 °C to 15% at 380 °C (Figure 4d). NO<sub>2</sub> selectivity is practically negligible regardless of temperature (Figure 4e).

In the absence of water, the distribution of products regarding reaction temperatures for the different zeolites is very similar, although at temperatures up to 300 °C the performance of chabazite is significantly superior, with higher N<sub>2</sub> selectivity and lower N<sub>2</sub>O and NO<sub>2</sub>

formation. In summary, Cu/CHA/M catalyst performs better than Cu/ZSM-5/M and Cu/BETA/M for the elimination of nitrogen oxides within the wide reaction temperature window with very high N<sub>2</sub> selectivity.

**Performance of coupled NSR (monolith) + SCR (granulated bed).** Figure 5 shows NO conversion and N<sub>2</sub>, NH<sub>3</sub>, N<sub>2</sub>O and NO<sub>2</sub> yields as a function of the reaction temperature in NSR-SCR experiments for SCR catalysts in granulated form, which have been placed after the NSR monolith. For comparison purposes, intermediate conversions at the exit of the NSR monolith are also shown (inverted triangles).

---

**Figure 5.** Conversion of NO, and N<sub>2</sub>, NH<sub>3</sub> and NO<sub>2</sub> yields during NSR and NSR-SCR reaction for monolith form NSR and powder form SCR catalysts.

---

As a general trend, the addition of an SCR catalyst downstream NSR catalyst significantly improved the NO conversion and N<sub>2</sub> production, eliminating completely the ammonia produced in the first stage, except at low reaction temperatures.

Among the prepared SCR catalysts, Cu/CHA showed NO conversion above 80% for all tested reaction temperatures, achieving almost full NO removal for reaction temperatures ranged between 200 and 250 °C. Interestingly, almost 100% NO conversions were accomplished for all tested reaction temperatures when water was present in the feedstream. In contrast, Cu/BETA and Cu/ZSM-5 catalysts only achieved 80% NO conversion at 250 and 200 °C, respectively. Moreover, chabazite also improves N<sub>2</sub> production (always higher than 70%), and emitted very low amount of NO<sub>2</sub> (<5%), overcoming the results obtained with ZSM-5 and BETA based catalysts.

The effect of 5% water addition to the feed significantly improves NO conversion of the NSR-Cu/CHA system (see Figure 5a). Despite the NO<sub>x</sub> removal improvement, not all the

ammonia supplied is used, and thus, some amount of  $\text{NH}_3$  is slipped to the atmosphere. This problem could be solved by using less amount of  $\text{H}_2$  during the rich period, allowing less  $\text{NH}_3$  generation in the NSR catalyst.

**NSR-SCR experiments in monolith + monolith form.** In order to study the availability of NSR-SCR technology for NO elimination in the practical application of Diesel engines, a monolith-monolith configuration needs to be studied. **Figure 6** shows NO conversions and  $\text{NH}_3$ ,  $\text{N}_2$ , and  $\text{NO}_2$  yields as a function of the reaction temperature in only-NSR and NSR-SCR experiments with both catalysts in their monolithic form. For this study, the SCR performance of Cu/CHA/M and Cu/ZSM-5/M was analyzed.

---

**Figure 6.** Conversion of NO and  $\text{N}_2$ ,  $\text{NH}_3$ , and  $\text{NO}_2$  yields during NSR and NSR-SCR reaction for monolith form NSR and SCR catalysts.

---

In this case, results qualitatively similar to coupled systems with granulated SCR catalyst are obtained. With respect to only-NSR (dashed line in Fig. 6), the double NSR-SCR disposition improved the NO conversion and  $\text{N}_2$  production with both catalysts, eliminating almost completely the ammonia generated during the NSR rich (reducing) period. Nevertheless, the NSR-Cu/CHA/M configuration resulted in better catalytic performance, with almost complete elimination of NO at low temperature and values above 80% for higher temperatures. In addition, this catalytic system achieves high  $\text{N}_2$  selectivity (above 80% for all reaction temperatures). Furthermore, neither  $\text{NH}_3$  nor  $\text{N}_2\text{O}$  and  $\text{NO}_2$  is practically emitted above 200 °C. In contrast, the NSR-Cu/ZSM-5/M system showed NO conversion not higher 85%, and high  $\text{N}_2$  production (~ 80%) is only achieved around 200 °C.

On the other hand, the addition of water to the feedstream has been studied in the final configuration using Cu/CHA/M as SCR catalyst (see Figure 6, red dashed lines). The NSR-

Cu/CHA/M system performed similarly to the same catalytic system in the absence of water. The main difference appears at temperatures below 200 °C, where less NO is converted to N<sub>2</sub> and more NH<sub>3</sub> is emitted to the atmosphere. These issues could be explained by the inhibition of the oxidation of NO to NO<sub>2</sub> in the NSR catalyst, which is the determining reaction rate at low temperatures, as it has been described above. Finally, high NO conversions are maintained at high temperatures, due to the inhibition of ammonia oxidation by the addition of water.

## CONCLUSIONS

In this study, the single-SCR, single-NSR and coupled NSR-SCR of NO<sub>x</sub> have been studied with NH<sub>3</sub>-SCR Cu/CHA, Cu/ZSM-5 and Cu/BETA, including the hydrothermal stability of the catalysts, the conversion of NO, slip of NH<sub>3</sub> and N<sub>2</sub>O and NO<sub>2</sub> yields.

XRD patterns of fresh and aged samples proved no collapse of the structure that remained largely intact. However, the aging under 5% steam/Ar at 750 °C for 16 h provoked uneven decrease in the surface area, micropore volume and acidity of the samples, resulting the Cu/CHA the more resistant structure, followed by Cu/ZSM-5 and then Cu/BETA. The lower dealumination of Cu/CHA allows maintaining practically unaltered the moderate acidity (NH<sub>3</sub> desorption peak centered at 250 °C) of the aged sample with respect to the fresh sample. On the other hand, the aging process was noted to include remarkable changes in the copper species distribution, CuO and Cu(II) exchanged on tetrahedral and octahedral positions of the zeolite framework, depending on the zeolite structure. Again, while the totally consumed H<sub>2</sub>-TPR for Cu/CHA remains almost unaltered after aging, in the case of Cu/ZSM-5 and Cu/BETA an additional peak at high temperature informs on migration of Cu from tetrahedral to octahedral framework positions.

The prepared granulated Cu/CHA, Cu/ZSM-5 and Cu/BETA samples were tested in the NO NH<sub>3</sub>-SCR reaction, in which NO conversion increases with temperature, it is maintained at intermediate temperature and then decreases at higher temperature when NH<sub>3</sub> oxidation is promoted, maintaining almost 100% selectivity to N<sub>2</sub> from 150 to 500 °C. However, Cu/CHA achieves superior performance with practically 100% NO conversion from 220 to 380 °C. The presence of water in the feedstream improves NO conversion at higher temperatures in all cases, probably because ammonia oxidation is inhibited by the presence of water, whereas small differences are observed in the low-medium temperature range. The excellent hydrothermal resistance of Cu/CHA is appreciated maintaining unaltered NO total conversion from 220 to 380 °C, which only decreased at higher temperature, in contrast with Cu/ZSM-5 and Cu/BETA that suffer from significant destruction of surface area, acidity and surface reducibility causing notable decrease in their catalytic performance. In all cases, a certain increase of N<sub>2</sub>O selectivity is noted at intermediate temperature, less than 10% in the case of Cu/CHA.

Comparison of the catalytic performance of the SCR catalysts when supported on the cordierite monolith (Cu/CHA/M, Cu/ZSM-5/M and Cu/BETA/M) follows the same trend as in their granulated form. In the case of Cu/CHA/M NO conversion over 90% is maintained in the 220-320 °C temperature range (somewhat narrower than with the granulated catalyst) which is even maintained when water is present in feedstream. However, the presence of water in the feedstream provokes progressive increasing of N<sub>2</sub>O selectivity with temperature from negligible at 140 °C to 15% at 380 °C, with the consequent loss of N<sub>2</sub> selectivity.

The prepared SCR catalysts were placed downstream a model monolith Pt-BaO/Al<sub>2</sub>O<sub>3</sub> catalyst, i.e. the so-called NSR-SCR technology, and the catalytic performance of the coupled system was analyzed. As expected, the coupled NSR-SCR system improves significantly NO conversion selectively to N<sub>2</sub> with eventually no slip of ammonia at the exit. NO conversion

profiles with temperature become flatter, extending the operation temperature windows regardless of the SCR catalyst. Best results are provided by Cu-CHA achieving 80% NO conversion and above from 150 to 400 °C, with some small ammonia slip only at lower temperature that disappears up to 200 °C. When water is present in the environment NO conversion is even enhanced up to 100% in the whole temperature range although less selectively to N<sub>2</sub> due to production of NH<sub>3</sub> (up to 20%) at temperature lower than 250 °C. We suggest that this problem could probably be overcome by tuning (decreasing) the amount of H<sub>2</sub> injected during the rich period of the cycle (this is now under detailed study by the authors).

Finally, focused on the real application, when testing the coupled NSR-Cu/CHA/M (both catalysts deposited on the cordierite monolith) the performance is slightly affected with respect to the granulated SCR catalyst in the absence of water. However, the presence of water in the feedstream does not enhance activity but even does inhibit NO activity at lower temperatures (< 220 °C) increasing the ammonia slip through the system. N<sub>2</sub>O is practically not emitted and a few NO<sub>2</sub> is emitted only at lower temperatures.

## ASSOCIATED CONTENT

### **Supporting Information**

The Supporting Information is available free of charge on the ACS Publications website at DOI: 10.1021/acscatal.XXXXXXX.

Physico-chemical characterization of prepared catalysts (Figures S1-S4).

## AUTHOR INFORMATION

Corresponding authors

\*E-mail: [juanra.gonzalezvelasco@ehu.es](mailto:juanra.gonzalezvelasco@ehu.es) (Juan R. González-Velasco)

\*E-mail: [acorma@itq.upv.es](mailto:acorma@itq.upv.es) (Avelino Corma)

#### ACKNOWLEDGEMENTS

The authors wish to acknowledge the financial support by the Spanish Economy and Competitiveness Ministry [CTQ2012-32899; MAT2012-3716, and “Severo Ochoa” (SEV 2012-0267)], the Basque Government (IT657-013), and the European Union (SynCatMatch project; ERC-AdG-2014-671093). One of the authors (UDLT) acknowledge to the Basque Government for the PhD Research Grant (BFI-2010-330).

#### REFERENCES

- [1] P. Granger and V.I. Parvulescu, *Chem. Rev.* **2011**, *111*, 3155.
- [2] N. Miyoshi, S. Matsumoto, T. Katoh, T. Tanaka, J. Harada, N. Takahashi, K. Yokota, M. Sugiara and K. Kasahara, *SAE Technical. Paper 950809*, **1995**.
- [3] W.S. Epling, L.E. Campbell, A. Yezerets, N.W. Currier and J.E. Parks, *Catal. Rev. Sci. Eng.* **2004**, *46*, 163.
- [4] B. Pereda-Ayo, R. López-Fonseca and J.R. González-Velasco, *Appl. Catal. A: Gen.* **2009**, *363*, 73.
- [5] L. Lietti, I. Nova and E. Tronconi, *Catal. Today* **1998**, *45*, 85.



- [6] E.C. Corbos, M. Haneda, X. Courtois, P. Marecot, D. Duprez and H. Hamada, *Catal. Commun.* **2008**, *10*, 137.
- [7] U. De La Torre, B. Pereda-Ayo, M. Romero-Sáez, A. Aranzabal, M.P. González-Marcos, J.A. González-Marcos and J.R. González-Velasco, *Top. Catal.* **2013**, *56*, 215.
- [8] H.S.Gandhi, J.V. Cavataio, R.H. Hammerle and Y. Cheng, Ford Global Technologies LLC, *US Patent 7,485,273*, **2009**.
- [9] M. Weibel, N. Waldbüsser, P. Wunsch, D. Chatterjee, B. Bandl-Konrad and B. Kruntzsch, *Top. Catal.* **2009**, *52*, 1702.
- [10] L. Xu, R. McCabe, M. Dearth and W. Ruona, *SAE Tech. Pap.2010-01-0305*, **2010**.
- [11] B. Pereda-Ayo, D. Duraiswami and J.R. González-Velasco, *Catal. Today* **2011**, *172*, 66.
- [12] L. Castoldi, R. Bonzi, L. Lietti, P. Forzatti, S. Morandi, G. Ghiotti and S. Dzwigaj, *J. Catal.* **2011**, *282*, 128.
- [13] I. Nova and E. Tronconi (Eds.), *Urea-SCR Technology for deNO<sub>x</sub> After Treatment of Diesel Exhausts*, Springer, New York, **2014**.
- [14] R. Martínez-Franco, M. Moliner, C. Franch, A. Kustov and A. Corma, *Appl. Catal. B: Environ.* **2012**, *127*, 273.
- [15] F. Gao, J. Kwak, J. Szanyi and C.H.F. Peden, *Top. Catal.* **2013**, *56*, 1441.
- [16] P.G. Blakerman, E.M. Burkholder, H.-Y. Chen, J.E. Collier, J.M. Fedeyko, H. Jobson and R.R. Rajaram, *Catal. Today* **2014**, *231*, 56.

- [17] D.W. Fickel, E. D'Addio, J.A. Lauterbach and R.F. Lobo, *Appl. Catal.* **2011**, *102*, 441.
- [18] U. Deka, I. Lezcano-González, B.M. Weckhuysen and A.M. Baile, *ACS Catalysis* **2013**, *3*, 413.
- [19] B. Pereda-Ayo, U. De-La-Torre, M.J. Illán-Gómez, A. Bueno-López and J.R. González-Velasco, *Appl. Catal. B: Environ.* **2014**, *147*, 420.
- [20] H. Kwak, D. Tran, S.D. Burton, J. Szanyi, J.H. Lee and C.H.F. Peden, *J. Catal.* **2012**, *287*, 203.
- [21] D. Wang, Y. Jangjou, Y. Liu, M.K. Sharma, J. Luo, J. Li, K. Kamasamudran and W.S. Epling, *Appl. Catal. B: Environ.* **2015**, *165*, 438.
- [22] L. Ma, Y. Cheng, G. Cavataio, R.W. McCabe, Lixin Fu and J. Li, *Chem. Eng. J.* **2013**, *225*, 323.
- [23] C.K. Seo, H. Kim, B. Choi, M.T. Lim, C.H. Lee and C.B. Lee, *Catal. Today* **211**, *164*, 507.
- [24] L. Xu and McCabe, *Catal. Today* **2012**, *184*, 83.
- [25] J. Wang, Y. Ji, G. Jacobs, S. Jones, D.J. Kim and M. Crocker, *Appl. Catal. B: Environ.* **2014**, *148-149*, 51.
- [26] S.I. Zones, *US Patent 4,544,538*, **1985**.
- [27] B. Pereda-Ayo, U. De La Torre, M. Romero-Sáez, A. Aranzabal, J.A. González-Marcos and J.R. González-Velasco, *Catal. Today* **2013**, *216*, 82.

- [28] B. Pereda-Ayo, R. López-Fonseca and J.R. González-Velasco, *Appl. Catal. A: Gen.* **2009**, *363*, 73.
- [29] F. Gao, E.D. Walter, N.M. Washton, J. Szanyi and C.H.F. Peden, *Appl. Catal. B: Environ.* **2015**, *162*, 501.
- [30] S. Kieger, G. Delahay, B. Coq and B. Neveu, *J. Catal.* **1999**, *183*, 267.
- [31] U. De La Torre, B. Pereda-Ayo and J.R. González-Velasco, *Chem. Eng. J.* **2012**, *207-208*, 10.
- [32] M.P. Ruggeri, T. Selli, M. Colombo, I. Nova and E. Tronconi, *J. Catal.* **2014**, *311*, 266.
- [33] A. Gossale, I. Nova, E. Tronconi, *Catal. Today* **2008**, *136*, 18.

## TABLES AND FIGURES CAPTIONS

**Table 1.** The prepared catalysts.

**Table 2.** Physico-chemical properties of the powdered catalysts, fresh and after severe hydrothermal aging under 5% H<sub>2</sub>O/Ar at 750 °C for 16 h, at a total flow rate of 600 ml min<sup>-1</sup>.

**Figure 1.** NO conversion, NH<sub>3</sub> conversion and N<sub>2</sub> selectivity during SCR reaction for the catalysts, in their granulated form (fixed bed reactor).

**Figure 2.** Conversion of NO, NH<sub>3</sub> and N<sub>2</sub> selectivity during SCR reaction for the catalysts in their granulated form in the absence (black) and presence (red) of water in the feed for a) Cu/CHA, b) Cu/BETA and c) Cu/ZSM-5 catalysts.

**Figure 3.** Conversion of NO, NH<sub>3</sub> and selectivity of N<sub>2</sub>, N<sub>2</sub>O and NO<sub>2</sub> during SCR reaction for fresh (black) and aged (red) granulated catalysts a) Cu/CHA, b) Cu/BETA and c) Cu/ZSM-5.

**Figure 4.** Conversion of NO and NH<sub>3</sub> (two upper graphics) and selectivity of N<sub>2</sub>, N<sub>2</sub>O and NO<sub>2</sub> (three bottom graphics) during SCR reaction for the prepared monoliths.

**Figure 5.** Conversion of NO, and N<sub>2</sub>, NH<sub>3</sub> and NO<sub>2</sub> yields during NSR and NSR-SCR reaction for monolith form NSR and powder form SCR catalysts.

**Figure 6.** Conversion of NO and N<sub>2</sub>, NH<sub>3</sub>, and NO<sub>2</sub> yields during NSR and NSR-SCR reaction for monolith form NSR and SCR catalysts.